

Magnetic anisotropy energies and metal-insulator transitions in monolayers of α -RuCl₃ and OsCl₃ on graphene

P. H. Souza,¹ D. P. de Andrade Deus,² W. H. Brito,^{3,*} and R. H. Miwa¹

¹*Instituto de Física, Universidade Federal de Uberlândia, C.P. 593, 38400-902, Uberlândia, MG, Brazil*

²*Instituto Federal de Educação, Ciência e Tecnologia de Goiás,
Departamento de Áreas Acadêmicas, Jataí, GO, Brazil*

³*Departamento de Física, Universidade Federal de Minas Gerais,
C. P. 702, 30123-970, Belo Horizonte, MG, Brazil*

(Dated: March 14, 2022)

Transition metal trichlorides, with $4d$ or $5d$ electrons, are materials at the forefront of recent studies about the interplay of spin-orbit coupling and strong Coulomb interactions. Within our first-principles calculations (DFT+ U +SOC) we study the effects of graphene on the electronic and magnetic properties of the monolayers of α -RuCl₃ and OsCl₃. Despite the spatially inhomogeneous n -type doping induced by graphene, we show that the occupancy of the upper Hubbard bands of MLs of α -RuCl₃ and OsCl₃ can be tuned through external electric fields, and allows the control of (i) metal-insulator transitions, and (ii) the magnetic easy-axis and anisotropy energies. Our findings point towards the tuning of electronic and magnetic properties of transition metal trichlorides monolayers by using graphene and external electronic fields.

I. INTRODUCTION

Magnetic interactions in correlated materials are well known for giving rise to new energy scales and emerging properties. In Mott insulators, with localized d -electrons, these interactions can give rise to an antiferromagnetic ground state,^{1,2} which upon hole doping leads to unconventional superconductivity.³ On the other hand, in f -electron materials the antiferromagnetic interaction between local moments and the conduction electrons leads to the Kondo effect and the appearance of strongly renormalized quasiparticles.⁴ More recently, the interplay of spin-orbit coupling (SOC), strong Coulomb and the emerging magnetic interactions has become of great interest since it can give rise to unusual electronic phases and nontrivial topology.^{5,6}

At the forefront of recent studies in this field are the $4d$ and $5d$ based materials, such as ruthenium and osmium compounds. In special, α -RuCl₃ has attracted great interest since it is a candidate for the realization of a Kitaev-like quantum spin liquid.⁷ However, this material is found to be a spin-orbit Mott insulator which orders antiferromagnetically at low temperatures.⁸ The intriguing magnetic interactions in α -RuCl₃ are also responsible for competing magnetic phases. More recently, several works have addressed the strength and nature of these interactions. For instance, recent X-ray scattering data have obtained a ferromagnetic Kitaev term in α -RuCl₃,⁹ in good agreement with previous calculations.^{10,11} Moreover, within density functional theory (DFT)+ U +SOC calculations, Kim *et al.*¹² found that a zigzag antiferromagnetic (ZZ-AFM) phase of α -RuCl₃ is slightly more stable than the FM configuration for U values between 1.0 and 3.5 eV, where the former is characterized by an energy gap of ~ 0.8 eV. Such a nearly degeneracy between FM and ZZ-AFM phases has been confirmed by recent works.^{13,14}

The monolayers (MLs) of the $4d$ and $5d$ transition metal trichlorides have also attracted great attention due to their magnetic and electronic properties. In the work of Huang *et al.*,¹³ the authors explored the quantum anomalous Hall (QAH) effect in monolayer of α -RuCl₃. However, instead of a semiconducting phase,¹² they found a semimetallic system even upon the inclusion of the SOC. In contrast, the semiconducting character of the ML α -RuCl₃ has been confirmed by recent calculations of Sarikurt *et al.*¹⁵, with energy gaps of about 0.7 eV (FM) and 1.0 eV (ZZ-AFM) for $U=2.0$ eV. From the experimental side, neutron scattering experiments¹⁶ indicated that single crystals of α -RuCl₃, with Ru³⁺ ($4d^5$) ions exhibit a ZZ-AFM configuration at low temperatures.

Similar magnetic phases have also been explored in the ML OsCl₃, which in contrast to α -RuCl₃, is predicted to be ferromagnetic.¹⁷ In addition, ML OsCl₃ has been considered as a candidate of a quantum anomalous Hall (QAH) insulator,¹⁷ although the Coulomb interactions counteract and favor the appearance of a Mott insulating phase. More recently, it was pointed out that the parent compound Os_{0.55}Cl₂ presents features of a quantum spin-liquid, with gapless magnetic fluctuations which prevent any magnetic ordering at low temperatures.¹⁸ Besides the feasibility of layered systems,¹⁹ and the prediction of Hubbard- U dependent QAH phase in the ML of OsCl₃,¹⁷ there are few works exploring its electronic and magnetic properties.

Another interesting property of these two-dimensional (2D) materials is their magnetic anisotropy energy (MAE). In the Ref. 15, the authors reported a MAE of ~ 18.8 meV with the easy axis parallel to the α -RuCl₃ surface. Further calculations confirmed the energetic preference for the in-plane magnetization, however they obtained a MAE of 0.80 meV/Ru-atom for the ZZ-AFM phase,²⁰ which is much smaller than that obtained in Ref. 15.

Previous reports have also explored different ways to modify the properties of these 2D magnets. In the case of α - RuCl_3 , strain and optically driven charge excitations can be used to induce magnetic phase transitions.^{14,20,21} Another interesting way is by interfacial interaction with graphene. In particular, it has been found that the interaction between graphene and ML α - RuCl_3 ²² can enhance considerably the Kitaev interactions in latter, whereas it also modifies the Fermi surface topology of the former.¹⁴ Rizzo *et al.*²³, for instance, found that interlayer charge transfer between the ML α - RuCl_3 and graphene gives rise to plasmon polaritons with high mobility.

In this work, we study the the electronic and magnetic properties of the MLs of α - RuCl_3 and OsCl_3 in presence of graphene (Gr); *i.e.* α - RuCl_3/Gr and OsCl_3/Gr heterostructures. We find a net charge transfer (of the order of $10^{13}/\text{cm}^2$) from graphene to the transition metal trichlorides, however inhomogeneously distributed on the α - RuCl_3 and OsCl_3 surfaces. The upper Hubbard bands of both α - RuCl_3 and OsCl_3 become partially occupied, giving rise to correlated metallic phases. More important, we demonstrate that graphene and external electric fields (EEFs) can be used to control the Ru-4*d* (Os-5*d*) occupancy, and as a result, induce (i) metal-insulator transitions, and (ii) tune MAE in both two dimensional magnets, where the graphene monolayer acts as reservoir for the electron/hole doping of the MLs. For instance, in the case of α - RuCl_3/Gr , we observe a change of easy axis (from out of plane to in plane) accompanied by an enhancement of the MAE by a factor of six under external electric fields of $0.2 \text{ eV}/\text{\AA}$. These findings suggest that the occupancies of MLs α - RuCl_3 and OsCl_3 Hubbard bands are essential to control the magnetization easy-axis and the corresponding magnetic anisotropic energies. This control can be achieved with the presence of graphene and external electric fields.

II. COMPUTATIONAL DETAILS

Our density functional theory calculations were performed within the Perdew-Burke-Ernzerhof generalized gradient approximation (PBE-GGA),²⁴ using projector augmented wave (PAW) potentials,²⁵ as implemented in the Vienna ab initio Simulation Package (VASP) code.^{26,27} The structural optimizations were done including van der Waals corrections (vdW-DF)²⁸ until the forces on each atom were less than $0.01 \text{ eV}/\text{\AA}$. A plane wave cut-off of 500 eV was used, and k -point meshes of $(15 \times 15 \times 1)$, and $(31 \times 31 \times 1)$ for total energy and projected density of states calculations, respectively. The α - RuCl_3 and OsCl_3 monolayers were simulated using a slab with $\sqrt{3} \times \sqrt{3}$ surface periodicity, which corresponds to eight Ru/Os-atoms per unit cell [Fig. 1(a)], and a vacuum region of 20\AA , separating a slab from its periodic images.

To treat the strong correlations related to electrons within Ru-4*d* (Os-5*d*) states, we employed the DFT+ U functional of Dudarev,²⁹ which takes into account the

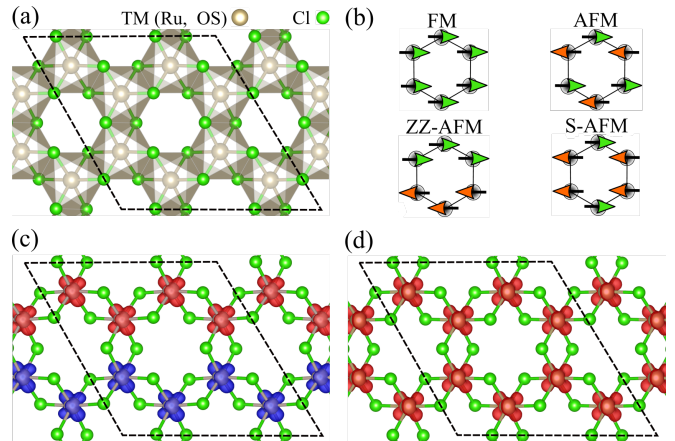


FIG. 1. (a) Layered honeycomb structures of the monolayers of α - RuCl_3 and OsCl_3 . (b) Distinct magnetic configurations associated with Ru(Os) local moments considered in our work. In (c) and (d) we show the spin density distributions corresponding to ZZ-AFM and FM phase of α - RuCl_3 and OsCl_3 , respectively. The red (blue) isosurfaces correspond to spin up (down) charge densities.

electronic interactions at a mean-field level by means of an effective partially screened Coulomb interaction U_{eff} . Likewise Refs. 22 and 17, we used values of $U_{\text{eff}} = U - J = 1.5 \text{ eV}$ and 1.0 eV for MLs of α - RuCl_3 and OsCl_3 , respectively. The spin-orbit coupling (SOC) was also taken into account in our calculations.

III. RESULTS AND DISCUSSIONS

A. Electronic and magnetic properties of MLs α - RuCl_3 and OsCl_3 within DFT+ U +SOC

The MLs of α - RuCl_3 and OsCl_3 have a two-dimensional honeycomb like structure, with slightly distorted TMCl_6 ($\text{TM} = \text{Ru}$, and Os) edge-sharing octahedra, as shown in Fig. 1(a). The corresponding crystal field splitting and occupancy of the Ru-4*d* (Os-5*d*) states lead to well defined local moments, which can order into distinct magnetic configurations. Within our DFT+ U +SOC approximation we investigate the relative energetic stability of several magnetic phases, *viz.*: ferromagnetic (FM), Néel antiferromagnetic (AFM), zigzag antiferromagnetic (ZZ-AFM), and stripy antiferromagnetic (S-AFM), which are schematically illustrated in Fig. 1(b).

In Table I we present the obtained total energy differences (ΔE) with respect to the lowest energy configuration, net magnetic moments (M), and band gaps (E_{gap}) of each magnetic phase. We find that ML α - RuCl_3 has a semiconducting ZZ-AFM ground state. The corresponding spin density, $\Delta\rho^{\text{spin}} = \rho_{\text{up}} - \rho_{\text{down}}$, shows a d_{xy} shaped $\Delta\rho^{\text{spin}}$ for the ZZ-AFM phase [Fig. 1(c)]. The local moment of $\approx 0.9 \mu_B/\text{Ru}$ atom is in good agreement

with previous reports,^{15,20} though, we obtain a distinct ground state magnetic configuration. From our calculations we find that ZZ-AFM is 4.5 meV/Ru-atom more stable than the FM state. In contrast, in the work of Sarikurt *et al.*,¹⁵ the FM state was found to be the ground state, with 20 meV/Ru-atom more stable than ZZ-AFM configuration. Further, Iyikanat *et al.* pointed out the ZZ-AFM configuration as the ground state configuration. According to these authors the energy difference between ZZ-AFM and FM configuration is around 0.8 meV/Ru-atom. This nearly degeneracy of ZZ-AFM and FM configurations was also reported in Refs. 12 and 14.

Moreover, the stripy (S-AFM) and Néel (AFM) configurations are around 9 and 12 meV/Ru less stable than the ZZ-AFM configuration, respectively. These small energy differences obtained within our approach reflect the competing energy scales presented in ML α -RuCl₃. In fact, as pointed out by Winter *et al.*³⁰ the rich phase diagram of α -RuCl₃ is ruled by competing Coulomb, kinetic and spin-orbit energy scales as well as long-range interactions, where the latter are very sensitive to the structural details. It turns out that ZZ-AFM ground state can be attributed to the presence of a large third-neighbor Heisenberg coupling between the Ru³⁺ local moments. Although the monolayer of α -RuCl₃ exhibits nearly degenerated magnetic configurations, the insulating nature of the system is preserved. In particular, the antiferromagnetic configurations have larger band gaps. For instance, the ZZ-AFM α -RuCl₃ has a band gap of around 200 meV larger than the FM configuration.

We next evaluate the magnetic anisotropy energy (MAE), which is defined as the total energy (E) difference of the α -RuCl₃, and OsCl₃ systems with the magnetization parallel (\parallel) and perpendicular (\perp) to the slab surface,

$$\text{MAE} = E_{\parallel} - E_{\perp}.$$

Here, the total energies E_{\parallel} and E_{\perp} were obtained by using the force theorem.³¹⁻³³ We found that the ZZ-AFM α -RuCl₃ presents an energetic preference for the out-of-plane (\perp) magnetization with MAE = 0.163 meV/Ru-atom. Meanwhile previous studies pointed out an energetic preference for the in-plane (\parallel) magnetization by 18.88 meV,¹⁵ and 0.80 meV/Ru-atom²⁰ for the FM and ZZ-AFM configurations, respectively.

As discussed above, the equilibrium geometry plays an important role in the magnetic properties of α -RuCl₃. Indeed, we found a subtle commitment between the atomic positions and the preferential orientation of the magnetic moment. We examined six slightly different equilibrium geometries obtained upon small perturbations on the initial (starting) atomic positions, and spin-configurations. We found that (i) the α -RuCl₃ systems with energetic preference for in-plane magnetization (MAE < 0) present Ru-Cl bonds lengths ($d_{\text{Ru-Cl}}$) with a nearly uniform distribution, characterized by a deviation ($\sigma_{d_{\text{Ru-Cl}}}$) of about 0.006 Å, whereas (ii) the ones with MAE > 0 present less uniform $d_{\text{Ru-Cl}}$ distribution, with $\sigma_{d_{\text{Ru-Cl}}} \approx 0.017$ Å. In all

cases, we found lowest energies in (ii) by ~ 30 meV/Ru-atom when compared with (i). Thus, providing further support to the energetic preference for the out-of-plane magnetization in α -RuCl₃.

TABLE I. Magnetic moments M (μ_B /TM-atom), relative energetic stabilities ΔE (meV/TM-atom), and band gaps E_{gap} (eV) of distinct magnetic configurations of α -RuCl₃ and OsCl₃ monolayers.

	M	ΔE	E_{gap}
α -RuCl ₃			
ZZ-AFM	0.89	0.0	0.74
FM	0.90	4.5	0.50
S-AFM	0.90	8.6	0.66
AFM	0.86	11.6	0.80
OsCl ₃			
ZZ-AFM	0.80	3.0	0.77
FM	0.92	0.0	0.54
S-AFM	0.83	12.5	0.62
AFM	0.72	5.13	0.75

In contrast to α -RuCl₃, the OsCl₃ presents a FM ground state followed by the ZZ-AFM configuration, which is higher in energy by 3.0 meV/Os-atom; both magnetic phases are characterized by an energetic preference for in-plane magnetization, with a sizeable MAE of -27.68 (FM) and -18.71 meV/Os-atom (ZZ-AFM). Our findings are in good agreement with Ref. 17, which reported on small energy difference between the FM and ZZ-AFM configurations, and in-plane magnetization. Similarly to α -RuCl₃, the spin density of FM OsCl₃ is centered around the transition metal atoms, as can be seen in Fig. 1(d), and poses a net magnetic moment of $0.9 \mu_B$ /Os-atom. The FM ground state exhibits a band gap of 0.54 eV, while the ZZ-AFM configuration has a gap of 0.77 eV.

The Mott insulating states of MLs of α -RuCl₃ and OsCl₃ monolayers are evidenced by the band structures and projected density of states shown in Fig. 2. In both materials, the gap appears due to the splitting of $j_{\text{eff}} = 1/2$ states in lower and upper Hubbard bands, which are originated from Ru(Os)- t_{2g} states. Moreover, from the projected density of states, one can notice that states from -1.6 to 1.2 eV are essentially formed by the Ru(Os)- d states, which are gapped due to interplay of SOC the Coulomb repulsion. In the case of ML OsCl₃, we also show the band structure of the ZZ-AFM configuration [Fig. 2(e)] has the same features of the RuCl₃(ZZ-AFM) [Fig. 2(a)]. The ground states of α -RuCl₃ and OsCl₃ exhibit band gaps of 0.74 and 0.54 eV (see table I), respectively. The former is in good agreement with previous calculations using small U values,²² although photoemission studies for bulk samples indicate values of around 1.9 eV.³⁴ It is worthy mentioning that in the case of ML OsCl₃, the neglecting of the Hubbard U term leads to a quantum hall anomalous insulating state with very small band gaps of ~ 67 meV.¹⁷

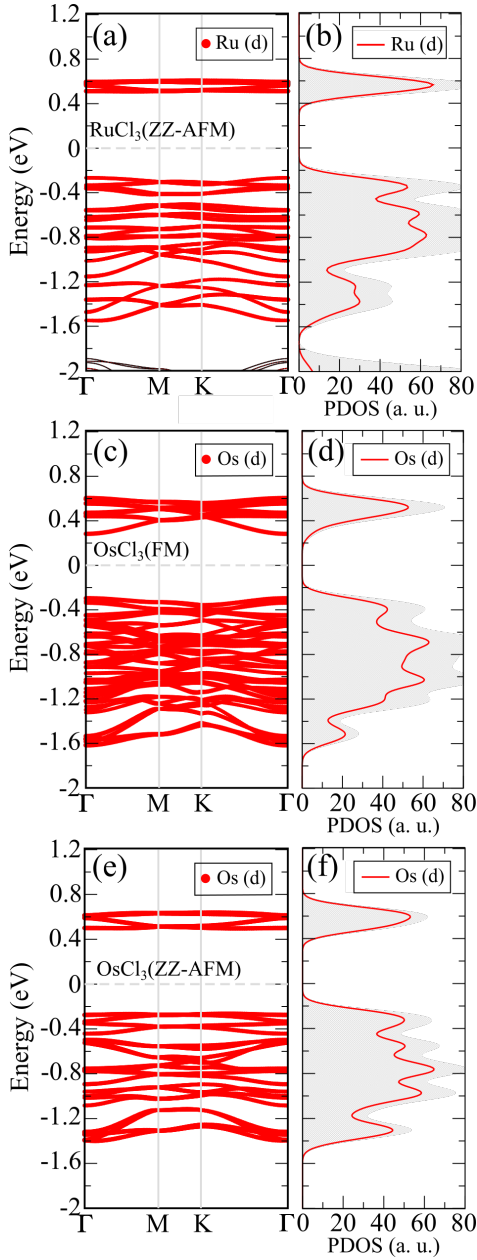


FIG. 2. DFT+ U +SOC band structures and projected density of states of the transition metal trichlorides monolayers: (a)–(b) RuCl_3 (ZZ-AFM), (c)–(d) OsCl_3 (FM), and (e)–(f) OsCl_3 (ZZ-AFM). Red lines represent the contribution from Ru-4 d (Os-5 d) states. The shaded regions in (b), (d) and (f) correspond to the total density of states.

B. Effects of graphene on α - RuCl_3 and OsCl_3

We now address the effects of graphene on the electronic and magnetic properties of both Ru and Os compounds. Van der Waals heterostructures have been employed as an alternative to tailor the properties of 2D materials without any drastic chemical or structural modification. For instance, graphene can be used to enhance

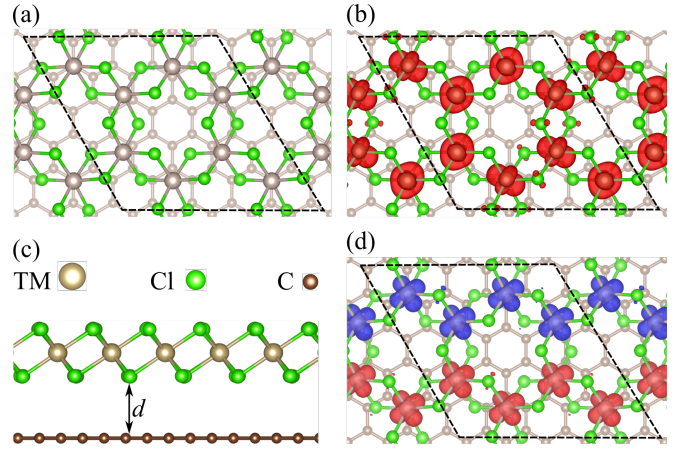


FIG. 3. (a) Optimized structural model of α - RuCl_3 /Gr and OsCl_3 /Gr. (b) Spin-resolved charge density isosurface corresponding to ferromagnetic phase of OsCl_3 /Gr. Similar spin-density is shown in (d) for α - RuCl_3 /Gr. (c) Side view of our optimized structure, where the interlayer distance $d = 3.6 \text{ \AA}$.

the Kitaev interactions and the spin-split of bands in the ML of α - RuCl_3 .^{22,35} To investigate the energetics and electronic structure of the monolayers of α - RuCl_3 and OsCl_3 on graphene, we perform structural optimizations of lattice parameters considering $\sqrt{3} \times \sqrt{3}$ hexagonal supercells, such as shown in Fig. 3(a). In the optimized structures the graphene lattice parameter is expanded by 0.84 % and 1.68 %, when interacting with α - RuCl_3 and OsCl_3 , respectively. In contrast, in Ref. 22 the authors kept the graphene lattice parameter fixed, with nearest neighbor distances of 1.42 \AA . Moreover, in our optimized structures the obtained interlayer distance between graphene and α - RuCl_3 (OsCl_3) is found to be around 3.6 \AA , as illustrated in Fig. 3(b). We evaluate the binding energy of both monolayers on graphene as follows,

$$E_b = \frac{E(\text{TMCl}_3/\text{Gr}) - E(\text{TMCl}_3) - E(\text{Gr})}{\text{Area}}, \quad (1)$$

where $\text{TM} = \{\text{Ru}, \text{Os}\}$. $E(\text{TMCl}_3/\text{Gr})$ is the total energy of our optimized structures, whereas $E(\text{TMCl}_3)$ denotes the total energy of monolayer of α - RuCl_3 (OsCl_3). $E(\text{Gr})$ is the total energy of graphene sheet. We find binding energies of -17.45 meV/\AA^2 and -16.47 meV/\AA^2 for α - RuCl_3 /Gr and OsCl_3 /Gr, respectively. It is important to mention that binding energy between graphene sheets are around -16.8 meV/\AA^2 .³⁶ These results emphasize the Van der Waals nature of interactions between the transition metal trichlorides and graphene. Therefore, it is unlikely that heterostructures made of transition metal trichlorides and graphene, exhibit considerable epitaxial in-plane strain values.

Next, we address the charge transfer between graphene and ML α - RuCl_3 (OsCl_3) by calculating the Bader charges of the heterostructures and the isolated systems as well. Our results are displayed in Table II. According

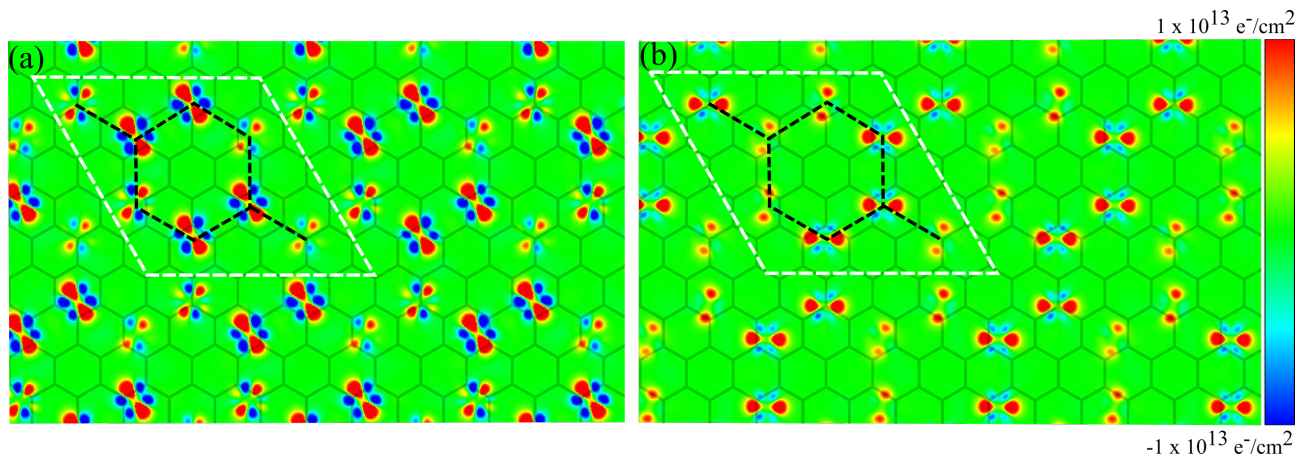


FIG. 4. In plane $\Delta\rho$ cut of isosurface associated with charge transfer from graphene to (a) α - RuCl_3 and (b) OsCl_3 monolayers. White dashed lines represent the supercells employed in our calculations. Black dashed lines show the hexagonal Ru and Os lattice to (a) α - RuCl_3 and (b) OsCl_3 .

to our findings, graphene donates $3.2 \times 10^{13} e/\text{cm}^2$ to α - RuCl_3 , and $2.1 \times 10^{13} e/\text{cm}^2$ to OsCl_3 . Roughly speaking, these results can be explained by the deep work function (Φ) of the transition metal trichlorides, which are 6.10 and 5.51 eV for single layer α - RuCl_3 and OsCl_3 , respectively, whereas $\Phi = 4.6$ eV for graphene.²³

TABLE II. Bader charges (in units of $e/\text{unit cell}$ ($\sqrt{3} \times \sqrt{3}$)) of isolated α - RuCl_3 (OsCl_3) and heterostructures with graphene. δ denotes the difference between the obtained charges of each isolated monolayer and in presence of graphene.

Atom	Charge (isolated)	Charge (on graphene)	δ
α - RuCl_3			
Ru	53.73	53.88	0.15
Cl	178.18	178.45	0.27
OsCl_3			
Os	52.91	53.00	0.09
Cl	179.01	179.19	0.18

In Fig. 4 we display the associated charge transfer map given by $\Delta\rho = \rho[\text{TMCl}_3/\text{Gr}] - (\rho[\text{TMCl}_3] + \rho[\text{Gr}])$, with $\text{TM} = \{\text{Ru}, \text{Os}\}$. In agreement with the obtained Bader charges, we find that graphene donates electrons to the transition metal trichlorides monolayers. Indeed, p -type doping of graphene in contact with α - RuCl_3 has been experimentally observed, and supported by *first-principles* DFT calculations.^{22,35,37} More interestingly, we observe an inhomogeneous electron doping of both α - RuCl_3 and OsCl_3 , which is more pronounced in the former [Fig. 4(a)]. Such inhomogeneous doping can be explained by the different hoppings between the TMCl_3 monolayer and the π -orbitals of the graphene sheet; which are sensitive to the stacking geometry at the α - RuCl_3 -Gr and OsCl_3 -Gr interfaces. These findings are consonance with the charge modulation as observed in recent Raman spectroscopy, and electronic transport

measurements.^{38,39} It is important to mention that inhomogeneous charge doping can be deleterious to the charge carriers transport in those systems, for instance, through the formation of electron-hole puddles,^{40,41} and have important effects on the magnetic interactions between the TM atoms within the distinct charge domains. It is worth noting that such an inhomogeneous net charge distribution, although less intense, has also been observed in OsCl_3/Gr , Fig. 4(b).

The interaction with graphene also gives rise to important effects on the electronic and magnetic properties of the transition metal trichlorides. As can be seen in Figs. 5(a) and (c), the donated electrons occupy the narrow upper Hubbard bands (UHB) of both α - RuCl_3 and OsCl_3 , giving rise to correlated metallic phases. As a result, graphene Dirac cone appears around 0.6 eV (0.5 eV) above the Fermi level in α - RuCl_3 (OsCl_3)/Gr, in good agreement with previous reports.^{22,23} This also can be observed in our calculated projected density of states shown in Figs. 5(b) and (d), where one can also notice the doping of the upper Hubbard bands. Besides the (partial) occupancy of the UHB, there is also a downshift of the high energy Ru(Os)- e_g like states in the presence of graphene. In fact, these states downshift by around 0.40 eV in α - RuCl_3 and 0.36 eV in OsCl_3 .

Focusing on the magnetic properties, we found that the ground state configuration of α - RuCl_3 , namely ZZ-AFM phase with out-of-plane magnetization, remains the same in α - RuCl_3/Gr . However, the total energy difference between the ZZ-AFM and FM configurations increases from 4.5 to 26.2 meV/Ru-atom, thus indicating that the energetic preference for the ZZ-AFM phase has been strengthened in α - RuCl_3/Gr . Meanwhile there is a reduction of the MAE from 0.163 to 0.118 meV/Ru-atom. On the other hand, in OsCl_3/Gr the ground state configuration of OsCl_3 changes from FM to ZZ-AFM, where the latter becomes more stable than the former by 8.19 meV/Os-atom. In both cases the energetic preference for the in-

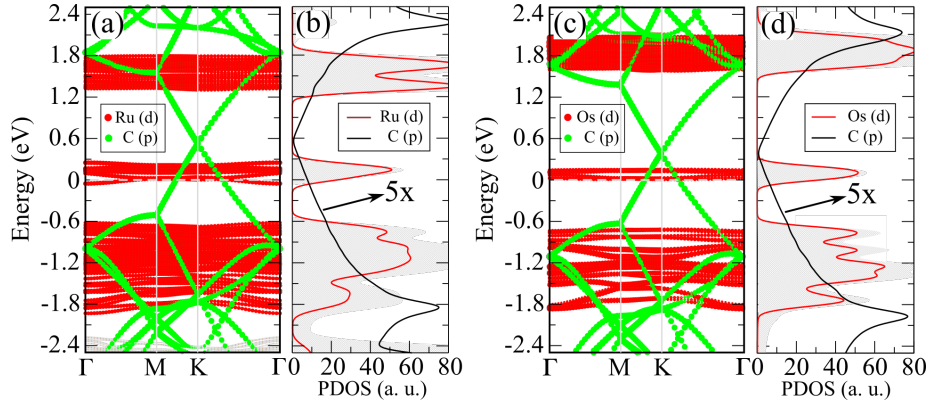


FIG. 5. Orbital resolved band structures and projected density of states of (a)–(b) α -RuCl₃/Gr and (c)–(d) OsCl₃/Gr. The Ru-4d (Os-5d) states are shown in red, whereas C-2p states are shown in green.

plane magnetization is maintained, however, somewhat similar to its counterpart, α -RuCl₃/Gr, there is a reduction of the MAE, *viz.*: $-27.68 \rightarrow -15.17$ meV/Os-atom (FM phase), and $-18.71 \rightarrow -14.04$ meV/Os-atom (ZZ-AFM). Since the structural changes on the α -RuCl₃ and OsCl₃ MLs due to their interaction with the graphene sheet are nearly negligible, we can infer that these changes (on the magnetic properties) are mostly dictated by the net charge transfer between graphene and the transition metal trichlorides. The role played by the $\text{Gr} \leftrightarrow \text{TMCl}_3$ charge transfers will be discussed in the next subsection.

As pointed out by Freeman and coworkers,⁴² the magnetic anisotropy energy depends on the relative position of occupied and unoccupied *d* energy levels, and on the coupling between them through the angular momentum operator \mathbf{L} . According to the authors, based on the second-order perturbation theory, the MAE can be estimated as follows,

$$\text{MAE} \approx \xi^2 \sum_{o,u} \left[\frac{|\langle o|L_z|u\rangle|^2 - |\langle o|L_x|u\rangle|^2}{\epsilon_u - \epsilon_o} \right], \quad (2)$$

for in-plane (out-of-plane) magnetization along the *x* (*z*) direction. ϵ_u and ϵ_o are the eigenvalues of the corresponding eigenstates, unoccupied (*u*) and occupied (*o*). Using the equation above, combined with the DFT+U+SOC calculations, we can have a detailed orbital understanding of the MAE results upon the formation of α -RuCl₃/Gr and OsCl₃/Gr interfaces.

Our orbital resolved MAE results, as displayed in Fig. 6, reveal that the out-of-plane magnetization of α -RuCl₃ is mostly dominated by the in-plane Ru-4d orbitals via the matrix element $\langle d_{x^2-y^2}|L_z|d_{xy}\rangle$, but there is also a contribution from out-of-plane orbitals, $\langle d_{z^2}|L_x|d_{yz}\rangle$, favoring the in-plane magnetization. As shown in Fig. 6(a), the values of the former term are larger than the latter one by 0.490 meV/Ru-atom. This energy difference between the matrix elements reduces to 0.413 meV/Ru-atom in α -RuCl₃/Gr [Fig. 6(b)], which is consistent with the reduction of MAE discussed above.

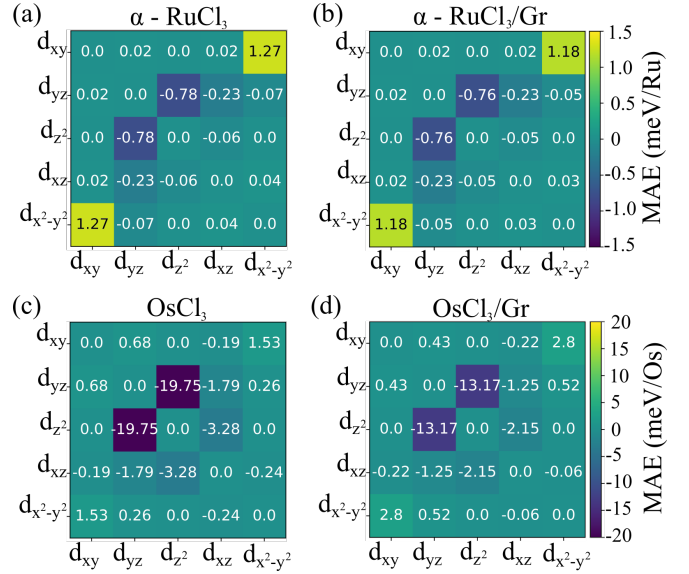


FIG. 6. Orbital resolved magnetic anisotropy energies (in meV/TM-atom) for (a) α -RuCl₃, (b) α -RuCl₃/Gr, (c) OsCl₃, and (d) OsCl₃/Gr. The blocks in our plots emphasize the contribution of the corresponding matrix elements.

The OsCl₃ and OsCl₃/Gr systems present a somewhat similar picture, where the matrix element $\langle d_{z^2}|L_x|d_{yz}\rangle$ dictates the energetic preference for in-plane magnetization, which in its turn reduces (by ~ 6.6 meV/Os-atom) upon the presence graphene sheet, as shown in Figs. 6(c) and (d).

C. Electric field induced metal-insulator transitions and control of magnetic anisotropy

The suitable control of the electronic and magnetic properties of materials by external agents, like mechanical pressure and electric field, is an important issue to the development of new electronic devices. For instance,

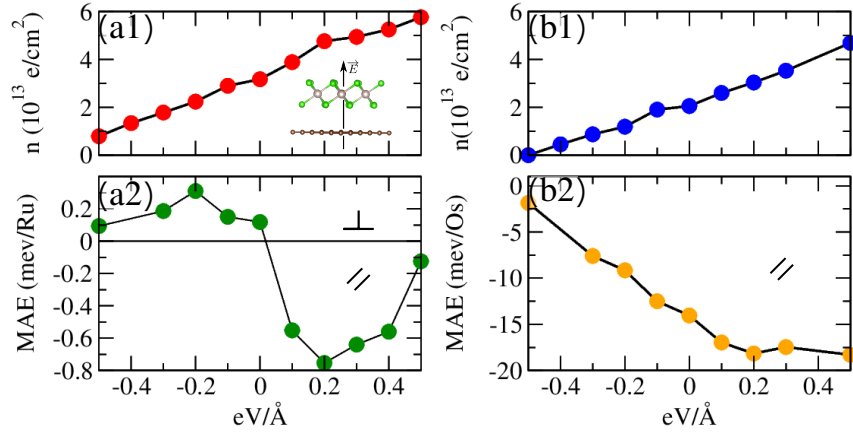


FIG. 7. Electron charge transfer as a function of an external electric field, for (a1) RuCl₃/Gr and (b1) OsCl₃/Gr. The direction of the external field is illustrated in the inset of (a1). In (a2) and (b2) we show the obtained MAEs for α -RuCl₃/Gr and OsCl₃/Gr, respectively. The parallel (||) and perpendicular (\perp) to the surface magnetizations are also indicated.

metal-insulator switching in transition metal oxides and intermetallic compounds,^{43–45} band alignment,^{46–48} control of the magnetic phases^{49,50} in 2D materials mediated by external electric field (EEF) and mechanical pressure.^{51,52} In the case of the α -RuCl₃/ and OsCl₃/Gr heterostructures, in addition to the Gr \rightarrow TMCl₃ electron doping (discussed above), we have also examined the effect of EEFs on the control of the net charge transfers, and on the magnetic/electronic properties as well.

As shown in Figs. 7(a1) and (b1), α -RuCl₃/Gr and OsCl₃/Gr heterostructures present nearly linear behavior of charge transfer as a function of the EEF. The n -type doping of the TMCl₃ MLs decreases upon negative values of EEF. For an EEF of about -0.65 eV/Å the electron transfer from graphene to α -RuCl₃ has been suppressed; likewise such a suppression occurs for EEF of ~ -0.50 eV/Å in the case of OsCl₃/Gr. In the opposite direction, one can increase the electron doping of TMCl₃ MLs mediated by positive values of EEF. For instance, for EEF of 0.3 eV/Å we find an electron doping of the α -RuCl₃ and OsCl₃ MLs of about $5.0 \times$ and 3.5×10^{13} electrons/cm², respectively. Therefore, the occupancy of the UHB can be controlled by the EEF, as can be seen in the band structures shown in Figs. 8(a) and (b). In particular, we observe insulating phases for α -RuCl₃ and OsCl₃ upon EEFs of -0.7 eV/Å and -0.5 eV/Å, respectively. The suppression of the charge transfers leads also to considerable downshift of the graphene's Dirac cone, as expected. As a result, metal-insulator transitions can be induced through external electric fields, which in its turn, controls the occupancy of the UHBs. Thus, our results demonstrate an alternative way to tune the $4d$ and $5d$ band filling in these compounds, and the magnetic properties of the TMCl₃ systems. Indeed, as shown in Figs. 7(a2) and (b2), the MAE of TMCl₃/Gr can be tuned by the EEF.

In Fig. 7(a2) we present the MAE of RuCl₃/Gr as a function of the EEF. It is noticeable that, (i) within

$|EEF| \leq 0.5$ eV/Å, the strength of the out-of-plane magnetization increases from 0.118 meV/Ru-atom ($EEF = 0$) to 0.311 meV/Ru-atom for an EEF of -0.2 eV/Å, corresponding to a reduction of the Gr \rightarrow RuCl₃ charge transfer, $\Delta\rho$, from $3.2 \times$ to 2.2×10^{13} e/cm². In contrast, (ii) the in-plane magnetization becomes energetically more favorable for positive values of the EEF, where we found MAE of -0.754 meV/Ru-atom for an EEF of 0.2 eV/Å. In this case, the n -type doping of RuCl₃ increases, with $\Delta\rho$ of 4.8×10^{13} e/cm².

We can gain further understanding of the role played by the EEF by analysing its effect on the (DFT+ U) orbital contribution to the MAE, eq. (2). Overall, we find that the orbital contributions to the MAE are reduced in comparison with those with no EEF. For instance, the out-of-plane contribution given by the matrix element $\langle d_{x^2-y^2} | L_z | d_{xy} \rangle$ reduces from 1.176 to 0.891 meV/Ru-atom, while the in-plane contribution via $\langle d_{z^2} | L_x | d_{yz} \rangle$ reduces (in absolute values) from 0.763 to 0.445 meV/Ru-atom. The larger energy reduction of the latter matrix element leads to an energetic preference for the out-of-plane magnetization, as discussed in (i). On the other hand, for EEF of 0.2 eV/Å [(ii)], the preference for in-plane magnetization, MAE = -0.754 meV/Ru-atom, is mostly ruled by the matrix element $\langle d_{x^2-y^2} | L_z | d_{xy} \rangle$ integrated over orbitals with opposite spins.^{33,42}

Meanwhile, the energetic preference for in-plane magnetization in OsCl₃/Gr is maintained within $|EEF| \leq 0.5$ eV/Å, Fig. 7(b2). There is an increase of the MAE from -14.04 meV/Os-atom ($EEF = 0$) to -18.16 meV/Os-atom for $EEF = 0.2$ eV/Å; in the opposite direction we find a nearly linear reduction of the MAE, $-14.04 \rightarrow -1.84$ meV/Os-atom, for negative values of EEF from 0 to -0.5 eV/Å. In the latter limit, the net charge transfer from graphene to OsCl₃ is suppressed, $\Delta\rho = 0$, suggesting that the preferential magnetization can be tuned from in-plane to out-of-plane mediated by higher values of EEF or p -type doping

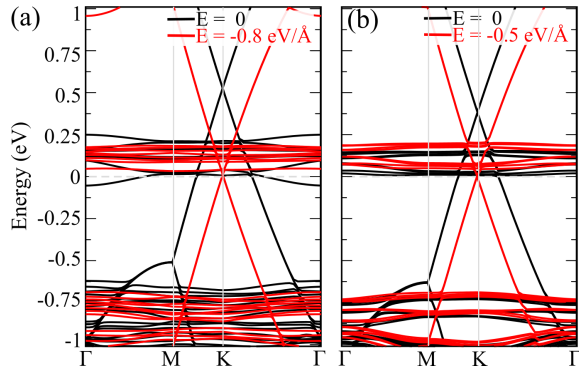


FIG. 8. Band structures of (a) α -RuCl₃/Gr and (b) OsCl₃/Gr, on the presence of an external electric fields of -0.8 eV/Å and -0.5 eV/Å, respectively. Bands shown in black (red) denote the calculated band structures without (with) an external electric field.

of the OsCl₃ ML. We have also examined the effect of EEF on the MAE in light of the perturbation theory. The calculated matrix elements, present in eq. (2), for EEF = 0.2 and -0.5 eV/Å, respectively, where we show that the MAE's changes as a function of the EEF are mostly ruled by the matrix elements $\langle d_{z^2} | L_x | d_{yz} \rangle$, and $\langle d_{z^2} | L_x | d_{xz} \rangle$. For instance, contribution from the former element increases/decreases from -13.165 (EEF=0) to $-15.139/-3.99$ meV/Os-atom for a EEF of $0.2/-0.5$ eV/Å.

It is worth noting that the changes on the MAE as a function of the EEF are dictated by the occupation of the Ru-4d and Os-5d orbitals, UHBs resonant or nearly resonant to the Dirac point. Thus, in order to stress the importance of the UHBs on the magnetization direction, we calculated the MAE of n -type (p -type) doped α -RuCl₃ (OsCl₃) ML. We found a magnetic transition from out-of-plane to in-plane, MAE = $0.163 \rightarrow -0.213$ meV/Ru-atom for $n = 1e$, in accordance with the energetic preference for the in-plane magnetization of α -RuCl₃/Gr upon EEF > 0 [Fig. 7(a2)]. Meanwhile, we find MAE = -16.41 meV/Os-atom in the p -type doped ($p = 0.033h$ upon an EEF of -0.7 eV/Å) OsCl₃ ML, confirming the tendency of change on the magnetic orientation, in-plane \rightarrow out-of-plane, for EEF < -0.5 eV/Å [Fig. 7(b2)]. Thus, our findings based on electron and hole doping of α -RuCl₃ and

OsCl₃ MLs, respectively, provide strong evidence that the occupation of the UHBs, indeed, play an important role on the tuning of the MAE.

IV. SUMMARY AND CONCLUSIONS

In summary, we performed DFT+ U +SOC calculations to investigate the effects of graphene on the electronic and magnetic properties of monolayers of α -RuCl₃ and OsCl₃, *i.e.* α -RuCl₃/Gr and OsCl₃/Gr heterostructures. We find that the α -RuCl₃ and OsCl₃ MLs become n -type doped, with n of the order of 10^{13} e/cm², characterized by an inhomogeneous spatial distribution of the net charge density, which depend on the stacking geometry (orbital hopping) between Ru(Os) and carbon atoms. The corresponding charge transfer gives rise to correlated metallic phases in both materials, mediated by the partially occupied upper Hubbard bands. We demonstrate that metal-insulator transitions can be induced in α -RuCl₃/ and OsCl₃/Gr using external electric fields, which in turn controls the occupancy of the Ru-4d Os-5d. More important, such control on the occupancies of the upper Hubbard bands leads to tuneable magnetic properties. We found that the in-plane magnetization becomes energetically favorable than the out-of-plane one in α -RuCl₃ upon n -type doping. Meanwhile, in the opposite direction, p -type doping of OsCl₃ results in an in-plane \rightarrow out-of-plane transition in the preferential magnetization direction. Our findings suggest that the occupancies of the Hubbard bands of the transition metal trichlorides are the key ingredients to tune the magnetic easy-axis as well as the magnetic anisotropy energies in these two-dimensional correlated materials. This tuning can be achieved with graphene and external electric fields.

ACKNOWLEDGMENTS

The authors acknowledge financial support from the Brazilian agencies CAPES, CNPq, FAPEMIG, and the National Laboratory for Scientific Computing (LNCC/MCTI, Brazil, project SCAFMat2) for providing HPC resources of the SDumont supercomputer, which have contributed to the research results, URL: <http://sdumont.lncc.br>.

* walber@fisica.ufmg.br

¹ N. F. Mott, *Metal-Insulator transitions*. Taylor & Francis, 2 ed., 1990.

² P. W. Anderson, "Antiferromagnetism. theory of superexchange interaction," *Phys. Rev.*, vol. 79, pp. 350–356, Jul 1950.

³ P. A. Lee, N. Nagaosa, and X.-G. Wen, "Doping a mott insulator: Physics of high-temperature superconductivity," *Rev. Mod. Phys.*, vol. 78, pp. 17–85, Jan 2006.

⁴ P. Coleman, *Heavy Fermions: electrons at the edge of magnetism*. In *Handbook of Magnetism and Advanced Magnetic Materials: Fundamentals and Theory (vol. 1)*, eds. H. Kronmüller and S. Parkin, John Wiley and Sons, 2007.

⁵ W. Witczak-Krempa, G. Chen, Y. B. Kim, and L. Balents, "Correlated quantum phenomena in the strong spin-orbit regime," *Annual Review of Condensed Matter Physics*, vol. 5, no. 1, pp. 57–82, 2014.

- ⁶ J. G. Rau, E. K.-H. Lee, and H.-Y. Kee, “Spin-orbit physics giving rise to novel phases in correlated systems: Iridates and related materials,” *Annual Review of Condensed Matter Physics*, vol. 7, no. 1, pp. 195–221, 2016.
- ⁷ L. J. Sandilands, Y. Tian, K. W. Plumb, Y.-J. Kim, and K. S. Burch, “Scattering continuum and possible fractionalized excitations in α - rucl_3 ,” *Phys. Rev. Lett.*, vol. 114, p. 147201, Apr 2015.
- ⁸ K. W. Plumb, J. P. Clancy, L. J. Sandilands, V. V. Shankar, Y. F. Hu, K. S. Burch, H.-Y. Kee, and Y.-J. Kim, “ α - rucl_3 : A spin-orbit assisted mott insulator on a honeycomb lattice,” *Phys. Rev. B*, vol. 90, p. 041112, Jul 2014.
- ⁹ J. A. Sears, L. E. Chern, S. Kim, P. J. Bereciartua, S. Francoal, Y. B. Kim, and Y.-J. Kim, “Ferromagnetic kitaev interaction and the origin of large magnetic anisotropy in α - rucl_3 ,” *Nature Physics*, vol. 16, p. 837, 2020.
- ¹⁰ S. M. Winter, K. Riedl, P. A. Maksimov, A. L. Chernyshev, A. Honecker, and R. Valentí, “Breakdown of magnons in a strongly spin-orbital coupled magnet,” *Nature Communications*, vol. 8, no. 1152, 2017.
- ¹¹ P. A. Maksimov and A. L. Chernyshev, “Rethinking α - rucl_3 ,” *Phys. Rev. Research*, vol. 2, p. 033011, Jul 2020.
- ¹² H.-S. Kim, V. S. V., A. Catuneanu, and H.-Y. Kee, “Kitaev magnetism in honeycomb rucl_3 with intermediate spin-orbit coupling,” *Phys. Rev. B*, vol. 91, p. 241110, Jun 2015.
- ¹³ C. Huang, J. Zhou, H. Wu, K. Deng, P. Jena, and E. Kan, “Quantum anomalous hall effect in ferromagnetic transition metal halides,” *Phys. Rev. B*, vol. 95, p. 045113, Jan 2017.
- ¹⁴ Y. Tian, W. Gao, E. A. Henriksen, J. R. Chelikowsky, and L. Yang, “Optically driven magnetic phase transition of monolayer rucl_3 ,” *Nano Letters*, vol. 19, no. 11, pp. 7673–7680, 2019. PMID: 31637915.
- ¹⁵ S. Sarikurt, Y. Kadioglu, F. Ersan, E. Vatansever, O. Ü. Aktürk, Y. Yüksel, Ü. Akinci, and E. Aktürk, “Electronic and magnetic properties of monolayer α - rucl_3 : a first-principles and monte carlo study,” *Phys. Chem. Chem. Phys.*, vol. 20, pp. 997–1004, 2018.
- ¹⁶ J. A. Sears, M. Songvilay, K. W. Plumb, J. P. Clancy, Y. Qiu, Y. Zhao, D. Parshall, and Y.-J. Kim, “Magnetic order in α - rucl_3 : A honeycomb-lattice quantum magnet with strong spin-orbit coupling,” *Phys. Rev. B*, vol. 91, p. 144420, Apr 2015.
- ¹⁷ X.-L. Sheng and B. K. Nikolić, “Monolayer of the $5d$ transition metal trichloride oscl_3 : A playground for two-dimensional magnetism, room-temperature quantum anomalous hall effect, and topological phase transitions,” *Phys. Rev. B*, vol. 95, p. 201402, May 2017.
- ¹⁸ M. A. McGuire, Q. Zheng, J. Yan, and B. C. Sales, “Chemical disorder and spin-liquid-like magnetism in the van der waals layered $5d$ transition metal halide $\text{os}_{0.55}\text{cl}_2$,” *Phys. Rev. B*, vol. 99, p. 214402, Jun 2019.
- ¹⁹ M. Grönke, P. Schmidt, M. Valldor, S. Oswald, D. Wolf, A. Lubk, B. Büchner, and S. Hampel, “Chemical vapor growth and delamination of α - rucl_3 nanosheets down to the monolayer limit,” *Nanoscale*, vol. 10, pp. 19014–19022, 2018.
- ²⁰ F. Iyikanat, M. Yagmurcukardes, R. T. Senger, and H. Sahin, “Tuning electronic and magnetic properties of monolayer α - rucl_3 by in-plane strain,” *J. Mater. Chem. C*, vol. 6, pp. 2019–2025, 2018.
- ²¹ D. S. Kaib, S. Biswas, K. Riedl, S. M. Winter, and R. Valentí, “Magnetoelastic coupling and effects of uniaxial strain in α - rucl_3 from first principles,” *arXiv:2008.08616v1*, 2020.
- ²² S. Biswas, Y. Li, S. M. Winter, J. Knolle, and R. Valentí, “Electronic properties of α - rucl_3 in proximity to graphene,” *Phys. Rev. Lett.*, vol. 123, p. 237201, Dec 2019.
- ²³ D. J. Rizzo, B. S. Jessen, Z. Sun, F. L. Ruta, J. Zhang, J.-Q. Yan, L. Xian, A. S. McLeod, M. E. Berkowitz, K. Watanabe, T. Taniguchi, S. E. Nagler, D. G. Mandrus, A. Rubio, M. M. Fogler, A. J. Millis, J. C. Hone, C. R. Dean, and D. N. Basov, “Charge-transfer plasmon polaritons at graphene/ α - rucl_3 interfaces,” *Nano Letters*, vol. 0, no. 0, p. null, 0. PMID: 33166145.
- ²⁴ J. P. Perdew, K. Burke, and M. Ernzerhof *Phys. Rev. Lett.*, vol. 77, p. 3865, 1996.
- ²⁵ P. E. Blüchl *Phys. Rev. B*, vol. 50, p. 17953, 1994.
- ²⁶ G. Kresse and J. Furthmüller *Comput. Mater. Sci.*, vol. 6, p. 15, 1996.
- ²⁷ G. Kresse and J. Furthmüller *Phys. Rev. B*, vol. 54, p. 11169, 1996.
- ²⁸ M. Dion, H. Rydberg, E. Schröder, D. C. Langreth, and B. I. Lundqvist, “Van der waals density functional for general geometries,” *Phys. Rev. Lett.*, vol. 92, p. 246401, Jun 2004.
- ²⁹ S. L. Dudarev, G. A. Botton, S. Y. Savrasov, C. J. Humphreys, and A. P. Sutton, “Electron-energy-loss spectra and the structural stability of nickel oxide: An lsd+u study,” *Phys. Rev. B*, vol. 57, pp. 1505–1509, Jan 1998.
- ³⁰ S. M. Winter, Y. Li, H. O. Jeschke, and R. Valentí, “Challenges in design of kitaev materials: Magnetic interactions from competing energy scales,” *Phys. Rev. B*, vol. 93, p. 214431, Jun 2016.
- ³¹ M. Weinert, R. E. Watson, and J. W. Davenport, “Total-energy differences and eigenvalue sums,” *Phys. Rev. B*, vol. 32, pp. 2115–2119, Aug 1985.
- ³² X. Wang, D.-s. Wang, R. Wu, and A. Freeman, “Validity of the force theorem for magnetocrystalline anisotropy,” *Journal of magnetism and magnetic materials*, vol. 159, no. 3, pp. 337–341, 1996.
- ³³ B. Yang, J. Zhang, L. Jiang, W. Chen, P. Tang, X.-G. Zhang, Y. Yan, and X. Han, “Strain induced enhancement of perpendicular magnetic anisotropy in co/graphene and co/bn heterostructures,” *Physical Review B*, vol. 95, no. 17, p. 174424, 2017.
- ³⁴ S. Sinn, C. H. Kim, B. H. Kim, K. D. Lee, C. J. Won, J. S. Oh, M. Han, Y. J. Chang, H. Hur, Namjung and Sato, B.-G. Park, C. Kim, H.-D. Kim, and T. W. Noh, “Electronic structure of the kitaev material α - rucl_3 probed by photoemission and inverse photoemission spectroscopies,” *Scientific Reports*, vol. 6, no. 39544, 2016.
- ³⁵ S. Mashhadi, Y. Kim, J. Kim, D. Weber, T. Taniguchi, K. Watanabe, N. Park, B. Lotsch, J. H. Smet, M. Burghard, and K. Kern, “Spin-split band hybridization in graphene proximitized with α - rucl_3 nanosheets,” *Nano Letters*, vol. 19, no. 7, pp. 4659–4665, 2019. PMID: 31241971.
- ³⁶ T. Gould, S. Lebègue, and J. F. Dobson, “Dispersion corrections in graphenic systems: a simple and effective model of binding,” *Journal of Physics: Condensed Matter*, vol. 25, p. 445010, oct 2013.
- ³⁷ E. Gerber, Y. Yao, T. A. Arias, and E.-A. Kim, “Ab initio mismatched interface theory of graphene on α - rucl_3 : Doping and magnetism,” *Physical Review Letters*, vol. 124, no. 10, p. 106804, 2020.

- ³⁸ B. Zhou, J. Balgley, P. Lampen-Kelley, J.-Q. Yan, D. G. Mandrus, and E. A. Henriksen, "Evidence for charge transfer and proximate magnetism in graphene- α -rucl 3 heterostructures," *Physical Review B*, vol. 100, no. 16, p. 165426, 2019.
- ³⁹ Y. Wang, J. Balgley, E. Gerber, M. Gray, N. Kumar, X. Lu, J.-Q. Yan, A. Fereidouni, R. Basnet, S. J. Yun, D. Suri, H. Kitadai, T. Taniguchi, K. Watanabe, X. Ling, J. Moodera, Y. H. Lee, H. O. H. Churchill, J. Hu, L. Yang, E.-A. Kim, D. G. Mandrus, E. A. Henriksen, and K. S. Burch, "Modulation doping via a two-dimensional atomic crystalline acceptor," *Nano Letters*, vol. 20, no. 12, pp. 8446–8452, 2020. PMID: 33166150.
- ⁴⁰ J. Martin, N. Akerman, G. Ulbricht, T. Lohmann, J. H. Smet, and K. Von Klitzing *Nat. Phys.*, vol. 4, p. 144, 2008.
- ⁴¹ R. H. Miwa, T. M. Schmidt, W. L. Scopel, and A. Fazzio *Appl. Phys. Lett.*, vol. 99, p. 163108, 2011.
- ⁴² D.-s. Wang, R. Wu, and A. J. Freeman, "First-principles theory of surface magnetocrystalline anisotropy and the diatomic-pair model," *Phys. Rev. B*, vol. 47, pp. 14932–14947, Jun 1993.
- ⁴³ R. Scherwitzl, P. Zubko, I. G. Lezama, S. Ono, A. F. Morpurgo, G. Catalan, and J.-M. Triscone, "Electric-field control of the metal-insulator transition in ultrathin ndnio3 films," *Advanced Materials*, vol. 22, no. 48, pp. 5517–5520, 2010.
- ⁴⁴ T. Zou, J. Peng, M. Gottschalk, P. P. Zhang, Z. Q. Mao, and X. Ke, "Insulator-metal transition induced by electric voltage in a ruthenate mott insulator," *Journal of Physics: Condensed Matter*, vol. 31, p. 195602, mar 2019.
- ⁴⁵ E. Janod, J. Tranchant, B. Corraze, M. Querré, P. Stollari, M. Rozenberg, T. Cren, D. Roditchev, V. T. Phuoc, M.-P. Besland, and L. Cario, "Resistive switching in mott insulators and correlated systems," *Advanced Functional Materials*, vol. 25, no. 40, pp. 6287–6305, 2015.
- ⁴⁶ E. S. Souza, W. L. Scopel, and R. Miwa, "Switchable magnetic moment in cobalt-doped graphene bilayer on cu (111): An ab initio study," *Physical Review B*, vol. 93, no. 23, p. 235308, 2016.
- ⁴⁷ J. Padilha, R. Miwa, A. J. da Silva, and A. Fazzio, "Two-dimensional van der waals pn junction of inse/phosphorene," *Physical Review B*, vol. 95, no. 19, p. 195143, 2017.
- ⁴⁸ R. B. Pontes, R. H. Miwa, A. J. da Silva, A. Fazzio, and J. E. Padilha, "Layer-dependent band alignment of few layers of blue phosphorus and their van der waals heterostructures with graphene," *Physical Review B*, vol. 97, no. 23, p. 235419, 2018.
- ⁴⁹ S. Jiang, J. Shan, and K. F. Mak, "Electric-field switching of two-dimensional van der waals magnets," *Nature materials*, vol. 17, no. 5, pp. 406–410, 2018.
- ⁵⁰ E. S. Morell, A. León, R. H. Miwa, and P. Vargas, "Control of magnetism in bilayer cri3 by an external electric field," *2D Materials*, vol. 6, no. 2, p. 025020, 2019.
- ⁵¹ T. Song, Z. Fei, M. Yankowitz, Z. Lin, Q. Jiang, K. Hwangbo, Q. Zhang, B. Sun, T. Taniguchi, K. Watanabe, *et al.*, "Switching 2d magnetic states via pressure tuning of layer stacking," *Nature materials*, vol. 18, no. 12, pp. 1298–1302, 2019.
- ⁵² D. d. A. Deus, I. de Oliveira, J. Oliveira, W. Scopel, and R. Miwa, "Magnetic and electronic switch in metal intercalated two-dimensional gep α_3 ," *arXiv preprint arXiv:2010.03591*, 2020.